Industrial Crops & Products 177 (2022) 114493

Contents lists available at ScienceDirect

Industrial Crops & Products

journal homepage: www.elsevier.com/locate/indcrop

Barrier packaging solutions from residual biomass: Synergetic properties of CNF and LCNF in films

Jon Trifol [a,b], Rosana Moriana [a,c,d,*]

[a] Department of Fibre and Polymer Technology, School of Engineering Sciences in Chemistry, Biotechnology and Health, KTH, Royal Institute of Technology, Teknikringen 56, 100 44 Stockholm, Sweden
[b] Department of Bioproducts and Biosystems, School of Chemical Engineering, Aalto University, P.O. Box 16300, FIN-00076 Aalto, Espoo, Finland
[c] Department of Molecular Sciences, SLU-Swedish University of Agricultural Sciences, Almas Allé 5, 750 07, Uppsala, Sweden
[d] Bioeconomy and Health Division, RISE-Research Institutes of Sweden, Drottning Kristinas Väg 61, Stockholm, Sweden

ARTICLE INFO

Keywords:
1 lignin containing cellulose nanofibers (LCNF)
2 cellulose nanofibers (CNF)
3 gas barrier properties
4 optical properties **5** antioxidant activity **6** mechanical properties

ABSTRACT

In this paper, for the first time, it is studied the synergetic properties of two different grades of nanocelluloses with different chemical compositions (cellulose nanofibrils-CNF with less than 1% of lignin and lignocellulose nanofibrils-LCNF with 16% of lignin). CNF and LCNF were mixed in different ratios to obtain bi-component films. Their performance in terms of transparency, bioactivity, thermo-mechanical and gas barrier properties was evaluated and compared with the performance of the neat CNF films. The presence of LCNF in the formulations conferred antioxidant and UV blocking properties to the films, as well as improved mechanical and barrier properties. Specifically, the incorporation of 25% LCNF to the CNF films increased the mechanical properties (94% increase in tensile stress and a 414% increase in strain at break) and decreased the water vapor transmission rate by 16% and the oxygen transmission rate by 53%. This performance improvement was attributed to the coexistence of nanocelluloses with different chemical composition and morphology. LCNF contributed to increment the interfacial adhesion between cellulose nanofibrils due to the presence of lignin and promote the creation of more tortuous paths for gas molecules. These synergetic properties shown by the CNF/LCNF bi-component films demonstrate high potential to be used as gas barrier packaging solutions.

1. Introduction

During last years, the concern regarding the environmental issues of our planet has boomed, as evidenced by the increased interest of the scientific community to replace petroleum feedstocks with renewable biomass to obtain energy and plastics (Baniasadi et al., 2021; Sorrentino et al., 2007) ¨. However, some of the main challenges to introduce bio-based packaging solutions into the market are still related to the cost, performance, and ethical issues derived from the use of crops traditionally proposed for food production. Residual biomass from agroforestry activities and industrial side-streams is a cheap source of organic carbon that may be proposed to design bio-based packaging materials without competing with the food value chain.(Trifol et al., 2021) However, more research is needed to overcome the identified performance drawbacks of using bio-based materials (i.e. low transparency, moisture resistance, gas barrier, and thermo-mechanical properties) as an alternative to traditional petroleum-based food packaging plastics.(Trifol et al., 2016b, 2016a).

Cellulose nanofibrils (CNF) are bio-based and biodegradable nanomaterials (Siró and Plackett, 2010) that have been proposed to be used for food packaging as stand-alone material (Azeredo et al., 2017), barrier coatings or as reinforcement of other biopolymers (Trifol et al., 2016a, 2016b). CNF are transparent (Trifol et al., 2017), show excellent mechanical properties, and superior oxygen barrier at low relative humidity (Abdul Khalil et al., 2016). However due to their high hydrophilicity and high water sorption, the oxygen permeability of CNF at high relative humidity can increase dramatically (Aulin et al., 2012; Fukuzumi et al., 2009; Minelli et al., 2010). Barrier properties are fundamental in food packaging applications, as the moisture and oxygen of the environment can enhance the degradation of the food (Trifol et al., 2016b, 2016a). Thus, strategies such as surface modification of nanocellulose (Missoum et al., 2013) or hybrid nanocellulose/nanoclay

* Corresponding author at: Department of Fibre and Polymer Technology, School of Engineering Sciences in Chemistry, Biotechnology and Health, KTH, Royal Institute of Technology, Teknikringen 56, 100 44 Stockholm, Sweden.
E-mail address: rosana.moriana.torro@ri.se (R. Moriana).

https://doi.org/10.1016/j.indcrop.2021.114493
Received 7 September 2021; Received in revised form 27 December 2021; Accepted 28 December 2021
Available online 3 January 2022

papers (Liu and Berglund, 2012) have been used to decrease the moisture sensitivity of CNF.

Traditionally CNF has been obtained from bleached pulp from different sources, but it can be also produce by other sources such as pine cone (Trifol et al., 2021), sisal fibers (Trifol et al., 2017), rapeseed straw (Svärd et al., 2019), or pineapple leaf fibers (Cherian et al., 2011). Recently it has been proposed to produce nanocelluloses from unbleached pulp instead of bleached pulp to keep the lignin in their composition and render the CNF more hydrophobic. LCNF have been also produced from softwood pulp(Horseman et al., 2017), pine cone (Trifol et al., 2021), and recycled old corrugated container (Amini et al., 2020) among others. Compared to CNF, LCNF have proved to offer extra functionalities than CNF (such as higher hydrophobicity, (Chen et al., 2018), antimicrobial properties against E. Coli (Georgouvelas et al., 2020; Yang et al., 2020), antioxidant (Trifol et al., 2021) and UV blocking properties (Bian et al., 2021)). So, they are a promising alternative material to CNF. However, LCNF materials also showed lower density (Horseman et al., 2017) and higher porosity (Amini et al., 2020) compared with CNF, which can be a drawback as properties such as mechanical properties and gas permeability are likely to depend on the density.

In our recent work (Trifol et al., 2021), pine cones, which are agro-food and forest residues, were integrally fractionated to recover different valuable hemicellulose/lignin and cellulose-rich fractions. LCNF with a 16% of lignin content and CNF with less than 1% of lignin were isolated from the cellulose-rich fraction. The potential of these nanocelluloses to be used as food packaging raw materials and as reinforcement of hemicellulose/lignin in composite films was assessed. Comparing nanocelluloses neat films, the presence of lignin in the LCNF films conferred bioactivity and an improved thermal and mechanical performance in terms of flexibility and tensile strength to the films. However, the LCNF neat films resulted in worse gas barrier properties that were ascribed to the decrease of the hydrogen bonds between and within the CNF and resulted in films with lower fiber density packaging and crystallinity. In this work, we propose to design bi-component nanocellulose-based films with different percentages of CNF and LCNF, to find the optimal LCNF content that allows to confer bioactivity to the films, at the same time that does not alter substantially the crystallinity and fiber packaging density of the CNF neat films. The suitability of mixing those CNF and LCNF to tune film performance as packaging material will be investigated in terms of synergetic properties between CNF and LCNF in different bi-component films.

2. Materials and methods

2.1. CNF and LCNF production

The isolation of LCNF and CNF from pine cones has been published elsewhere (Trifol et al., 2021). Briefly, pine cones were pre-treated under alkaline conditions (NaOH 1,5 M, 110 °C, 1 h) and afterwards were submitted to soda pulping (NaOH 1 M, 155 °C,3 h). Then, two different bleaching procedures were used to achieve LCNF and CNF. To obtain CNF a hard bleaching with $NaClO_2$ was performed, but to obtain LCNF a soft bleaching with H_2O_2 was used instead. Then the pulps were submitted to homogenization (M110EH Microfuidic processor), one pass in a 400–200 μm chamber and another 4 in a 200–100 μm chamber. After that, cellulose nanofibrils with less than 1% of lignin (CNF) and with 16% of lignin (LCNF) in their composition were obtained. CNF showed a diameter of 14.6 + /- 10.8 nm, while LCNF a diameter of 21.9 + /- 10.5 nm. (Trifol et al., 2021).

2.2. Film preparation

0.9 wt% LCNF and CNF suspensions were homogeneously mixed under vigorous magnetic stirring for 2 h and at 40 °C. Different formulations with an LCNF content of 25,50, and 75 wt% were ultrasonicated for 15 min and film cast in a 6 cm petri dish. The suspension was dried at room temperature for 7 days and labeled as CNF/LCNF XX, where XX stands for the wt% of LCNF in the composition. The chemical composition of the proposed film formulations is shown in Table 1.

2.3. Thermogravimetry analysis (TGA)

The thermal behavior of the films was evaluated by TGA in a nitrogen (50 mL/min) atmosphere. Briefly, 3–5 mg of dried material was run at least by duplicate in a Mettler Toledo TGA/DSC 1 STAR in the range of 25–800 °C at 10 °C/min (Oinonen et al., 2016). The onset (initial degradation temperature) was determined from the first local maximum in the second derivative thermogravimetric curve and down to the zero levels of the DTG axis using STAR eEvaluation Software (Mettler-Toledo, Columbus, OH). All measurements were run in triplicate.

2.4. X-ray diffraction (XRD)

The crystalline structure of the materials was investigated via X-ray diffraction. Patterns of the composites were obtained by using a Bruker CCD-Apex apparatus equipped with an X-ray generator (Ni-filtered Cu-Ka radiation). The analysis was performed at 40 kV and 40 mA, and a 0.06 °C step size in the range of 5°− 40° with a 0.06° step. The crystalline index (CI) was estimated by using the empirical method proposed by (Segal et al., 1959):

$$C.I. = \frac{I200 - Iam}{I200} * 100 \quad (1)$$

where I_{200} corresponds to the maximum intensity of the reflection plane 200 (around 2θ=22°), being I_{am} minimum intensity from the amorphous part of the sample (about 2θ=18°).

2.5. Mechanical properties

The materials' mechanical properties (tensile strength, strain, and modulus) were measured in an Instron Universal Testing Machine Model 5944 (Instron Engineering Corporation, Canton, MA) equipped with pneumatic jaws and a 250 N cell. The samples were cut into (5 × 50 mm) specimens, and five specimens were tested for each sample. The initial distance between the grips was 20 mm, and the strain rate of the grips was 2 mm min^{-1}. The samples were preconditioned at 23 °C and 50% RH overnight prior to the test.

2.6. Moisture uptake

The moisture uptake of the samples was calculated at least from two different specimens. Briefly, samples of 50 mg were preconditioned at 23 °C and 50% and weighted, and then they were dried at 105 °C overnight and weighted again. The difference between the two weights is the water uptake (Trifol et al., 2017).

2.7. Water vapor transmission rate (WVTR)

The WVTR of the films at 23 °C and 50% RH was measured by duplicate using $CaCl_2$ as a desiccant agent. Briefly the films were placed in a cup with a cross section (S) of 5 cm^2 and $CaCl_2$ as desiccating agent. Then the cup was placed under controlled atmosphere and the cup was weighted every hour. The mass increase of the cup was plotted against time and the slope of the regression line was (n) was obtained. The calculated WVTR is dependent on the film thickness so this value was normalized to 100 μm. Therefore the WVTR mas multiplied by the thickness (l) and divided by 100 (Tsuji et al., 2006) to obtain the WVTR of a 100 μm equivalent film (Trifol et al., 2021). The WVTR of a 100 μm equivalent film was calculated as:

Table 1
Estimation of the chemical composition of the proposed formulations.

	Ash[a]	Lignin[b]	Glucose[c]	Hemicellulose[c]	Arabinose[c]	Galactose[c]	Xylose[c]	Mannose[c]
CNF	1.4 + /- 0.6%	1.0 + /- 0.5%	73 + /- 3%	25 + /- 1%	10 + /- 0%	6 + /- 1%	37 + /- 1%	46 + /- 1%
CNF/LCNF 25	1.3 + /- 0.6%	4.7 + /- 1.3%	70 + /- 3%	24 + /- 1%	9 + /- 0%	6 + /- 1%	38 + /- 0%	47 + /- 1%
CNF/LCNF 50	1.2 + /- 0.5%	8.6 + /- 2.0%	67 + /- 3%	23 + /- 1%	8 + /- 0%	6 + /- 1%	38 + /- 0%	48 + /- 1%
CNF/LCNF 75	1.1 + /- 0.4%	12.2 + /- 2.7%	64 + /- 2%	22 + /- 1%	7 + /- 0%	5 + /- 1%	39 + /- 0%	49 + /- 0%
LCNF	1.0 + /- 0.3%	15.9 + /- 3.5%	61 + /- 2%	21 + /- 0%	6 + /- 0%	5 + /- 1%	39 + /- 0%	50 + /- 0%

[a] The ash content of each sample was determined by thermogravimetric analysis (TGA) in a Mettler Toledo TGA/DSC 1 STAR under N2 (50 mL/min) and O_2 (50 mL/min) (Tagami et al., 2019).
[b] TAPPI test method T222 om-06 (TAPPI, 2006) was followed to calculate the Klason lignin content of all the samples.
[c] The released monosaccharides of the hydrolysis of the klason lignin were then diluted in a 1:10 ratio filtered and evaluated using high-pH anion-exchange chromatography with pulsed amperometric detection (HPAEC-PAD Dionex ICS-3000 (Dionex Corp., USA). The eluents use in the HPAEC-PAD were 260 mM NaOH, 170 mM acetate, and Milli-Q water as the mobile phase. Neutral sugars (glucose, mannose, xylose, arabinose, galactose, rhamnose, galacturonic acid, and glucuronic acid) were considered as standards. Cellulose was estimated from the glucose content and the rest of hemicelluloses from their corresponding monomer.

$$\mathrm{WVTR} = \mathrm{n} * \frac{1/100}{\mathrm{S}} \tag{2}$$

2.8. Oxygen transmission rate (OTR)

The oxygen transmission rate of the films at 23 °C was determined using a MOCON OX-TRAN TWIN (Modern Controls Inc., Minneapolis, MN) equipped with a coulometric sensor following ASTM standard D3985–8 (ASTM 2005) using a mask of 5 cm^2 at atmospheric pressure (760 mmHg). The measurements were conducted at 23 °C, and 50% RH and the materials were conditioned overnight prior to the measurements. The OTR was normalized to film thickness.

2.9. Optical properties and UV-blocking behavior

The optical properties (transparency and haze) were analyzed via UV-Vis spectroscopy using a Shimadzu UV-250 (Shimadzu Corporation, Japan) equipped with an integrating sphere. The measurements were done in the range of 210–800 nm, and the measurement of haze was made according to the instruction of the manufacturer (Shimazdu Corporation, 2016):

The haze was determined as

$$Haze \quad (\%) = 100 * \frac{DIFFUSE \quad TRANSMITTANCE}{TOTAL \quad LIGHT \quad TRANSMITTANCE} \tag{3}$$

2.10. Antioxidant properties

The antioxidant properties were investigated by DSC (Mettler Toledo) in an oxidative atmosphere under dynamic conditions (España et al., 2012). This technique has previously shown comparable results to the antioxidant properties evaluated via other techniques such as ABTS or DHPP (Tagami et al., 2019). Briefly, approximately 4 mg of material was placed in a DSC crucible and heated from 30 °C to 350 °C at 5 °C/min under an oxygen atmosphere (50 mL/min).

2.11. Density

A piece of film of 2 cm × 2 cm was kept at 23 °C and 50% for 24 h and then the dimensions (thickness, width and length) and weight were measured. The density was calculated by dividing the weight by the volume.

3. Results and discussion

In previous study (Trifol et al., 2021), CNF and LCNF suspensions obtained from pine cones were used as reinforcing agents of hemicellulose/lignin biopolymers, conferring film forming capabilities to these biopolymers. In this study, it is proposed to evaluate the potential of bi-component CNF/LCNF films as a packaging material and elucidate the influence of the lignin in the film performance and functionality. Neat CNF and LCN suspensions, as well as all the CNF/LCNF formulations showed good film-forming ability, resulting in self-standing, uniform, and transparent films with a thickness ranging from 70 to 110 μm and a standard deviation of around 3 μm (Fig. 1). The increment of the LCNF content in the formulations made the films become yellowish and more translucent due to the increasing lignin content shown in Table 1.

The characteristics of all the developed films were evaluated in terms of crystallinity, thermal properties, gas permeability, antioxidant and optical properties and mechanical performance. Specifically, high mechanical strength and flexibility together with high thermal stability, as well as low gas permeability can bring important target properties for applications such as packaging films (Hansen and Plackett, 2008) Crystallinity is well-known to have major effects on mechanical and gas barrier properties, so the crystallinity index (C.I) of all the samples were evaluated by XRD. Fig. 2A displays the XRD patterns of all the films where main peaks at 15–16° and 22°, typical of type I cellulose were detected. The C.I of the films decreased with increasing content of LCNF due to the higher amorphous lignin content in their composition.

One of the main drawbacks of using biomass for creating packaging films is its high thermal sensitivity. Thus, the study of the thermal degradation of bio-based films is an important aspect for deciding processing parameters and for designing the utilization conditions of the final products. In this study, all the developed films were characterized by TGA. Fig. 2B shows the first-derivative thermogravimetric curves of all the film samples. Comparing the nanocellulosic pure samples, the LCNF displayed slightly higher thermal stability than the CNF samples and the onset values of all the bi-component films were between those values (i.e., between 280 °C and 270 °C). These values are coincident with reported values for untreated CNF and ensure their use in application where thermal processing temperatures of 200 °C are required (hot-pressing, spray drying, coatings dried at high temperature, extrusion.).

The potential of these bi-component films for active food packaging was evaluated by assessing the film antioxidant and optical properties (Fig. 2C, D and E). The antioxidant properties were investigated by calculating the onset temperature values from the DSC oxidative thermograms (España et al., 2012) (Fig. 2C). Oxygen enhances microbial degradation, therefore a material that has antioxidant properties can improve the shelf-life of the food. All the lignin-containing materials displayed a higher onset temperature when compared with CNF, indicating a higher resistance of LCNF to oxidative decomposition. The lignin richness in phenolic hydroxy groups conferred to the films antioxidant properties and therefore, inhibited the combustion/oxidation (España et al., 2012)(Catignani and Carter, 1982). Additionally, it can be observed how CNF/LCNF 25 has slightly higher antioxidant capabilities than the rest of the bi-component films. In Fig. 2D and E, the UV-Vis spectra of the films is shown, from where the transparency in the visible spectra and the UV-shielding behavior can be quantitatively evaluated by transmittance. Briefly, the UV-Vis spectrum is composed of

Fig. 1. Aspect of the films. From left to right: CNF, CNF/LCNF 25, CNF/LCNF 50, CNF/LCNF 75, LCNF.

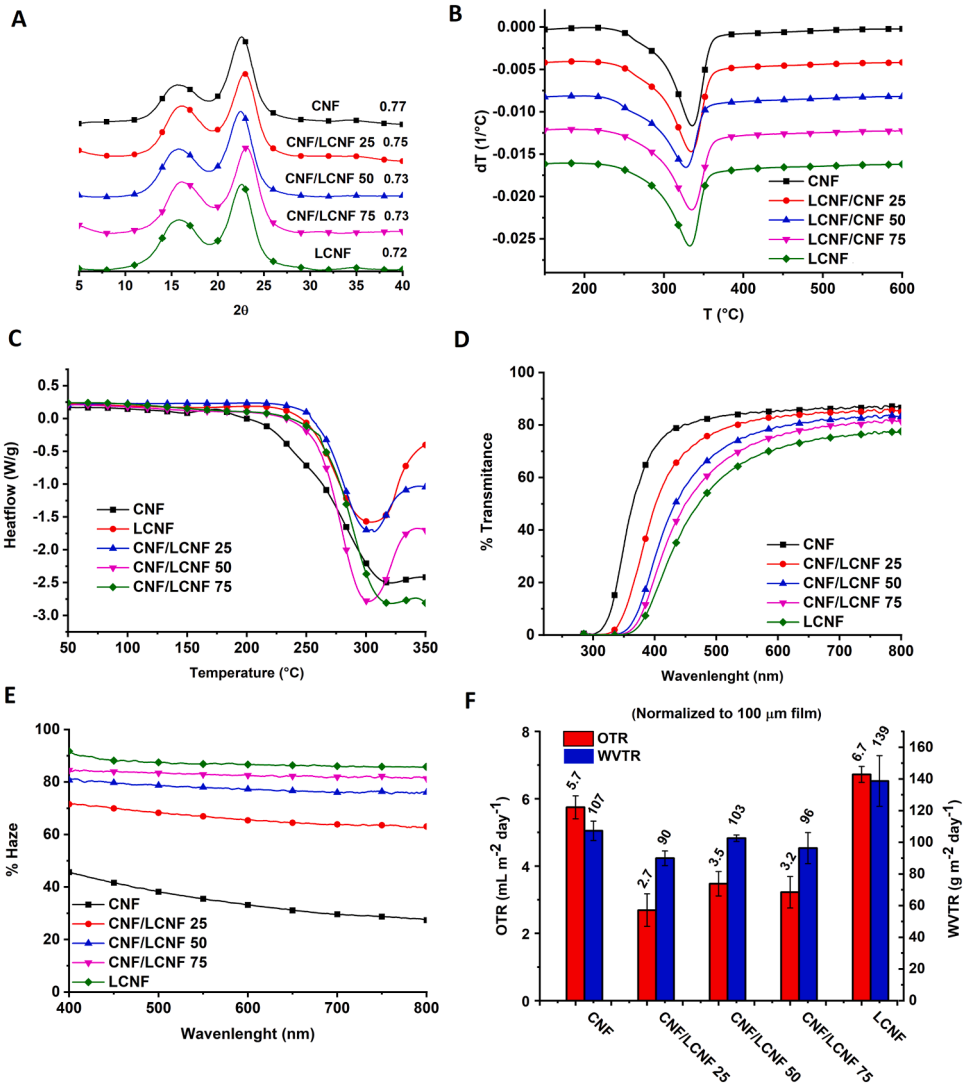

Fig. 2. Characteristics of the neat and bi-component films. A) XRD patterns of the films. B) first-derivative thermogravimetric curves of the films C) DSC film curves (O_2 atmosphere) D) Transmittance curves of the films. E) Haze calculated curves for all the studied films. F) Oxygen and water vapor transmission rates of the developed films (normalized to 100 μm).

the visible region (400–800 nm) and UV region (100−400) that is divided into UV-A (320–400 nm), UV-B (280–320 nm) and UV-C (100–280 nm) (Mehta and Kumar, 2019). Food packaging needs to protect food from light and UV radiation to avoid its chemical spoilage, however consumers usually demand transparent packages. Therefore, the ideal food packaging material should show high transparency in the visible region while low transparency in the UV region (Trifol et al., 2019, 2016b).

As can be seen from Fig. 2D, CNF showed some transparency in the UV-A (33% at 350 nm) and UV-B (4,5% at 320 nm) regions. However, bi-component films showed a high reduction in transmittance in both UV-A and UV-B regions (CNF/LCNF 25 showed 8% and 0,3% transmittance at 350 and 320 nm; – a 75% and a 94% reduction compared to neat CNF). This reduction in transmittance in the UVA and UVB regions increased as a function of the lignin content in the films. Therefore, all the designed bi-component films may be defined as high performance UV-blocking materials. Besides, LCNF neat films showed an even larger UV-blocking behavior, showing transmittances of 0,3% and 0% respectively at the aforementioned wavelengths. Therefore, it can be concluded that bi-component films have UV-blocking capabilities, and that the UV-blocking strength can be tuned by controlling the LCNF amount present in the films.

Another appealing function for packaging is their high transparency, which provides customers with a clear visibility of the content inside. In

the visible regions, the films with higher content of LCNF (>25%) displayed a slow increase of the transmittance from 400 to 600 nm until reaching a plateau at transmittance values of around 83% and 76% for the CNF/LCNF 50 and CNF/LCNF 75 films, respectively. When comparing CNF and CNF/LCNF 25, it can be noted that between 400 and 450 nm (blue/violet spectra) CNF has higher transparency, and above 450–500 nm both materials show similar behavior; at 450 nm, 80% transmittance vs. 70% transmittance and at 500 nm 83% vs. 77%. Therefore, CNF films only displayed higher transparency than the CNF/LCNF 25 in the range associated with the blue-violet colors within the visible spectrum. Considering that materials for food packaging needs to have both light transmittance and UV-blocking property, CNF/LCNF 25 was the optimal formulation to develop films in terms of optical properties.

Fig. 2E displays the haze parameter from 400 to 800 nm for all the films. As observed in Fig. 2C, the CNF neat films showed the highest transparency and, therefore, the lowest haze. In general, the films displayed lower haze at higher wavelengths. However, this trend is less significant in films with higher lignin content. CNF films had a decrease in their haze of 17% from 400 to 800 nm, however, LCNF displayed a haze decrease of only 7% at the same wavelength range. This is probably either due to the presence of lignin or due to the smaller diameter of CNF, allowing a better packaging of the fibrils, hence reducing the internal porosity of the materials – which may scatter the light.

Packaging films need to be impermeable for gases such as oxygen and water vapor to prevent the deterioration of food. Fig. 2F summarizes and compares the oxygen transmission rate and water vapor transmission rate (OTR and WVTR, respectively) of all the developed films. All the bi-component films displayed lower WVTR and OTR values than both neat films. Both LCNF and CNF neat films displayed gas transmission values in the range of the literature for nanocellulose films (Herrera et al., 2018; Lavoine et al., 2012; Rojo et al., 2015), showing high potential to be used for modified atmosphere packaging (MAP) for fruits and vegetables (Rodionova et al., 2011). In addition, the gas barrier properties shown by these bi-component films were better than the nanocellulose-based composites made from the same types of CNF and LCNF in the previous study (Trifol et al., 2021). In general, these values were less or similar than those of ethylene vinyl alcohol, polyamide 6, polystyrene, low density polyethylene, polyvinyl chloride, polylactic acid and cellulose-based films of similar thickness (Le Normand et al., 2014; Li et al., 2016; Oinonen et al., 2016; Schmid et al., 2012). Specifically, CNF/LCNF 25 films showed the best permeability values: The OTR was reduced by 53% and 60% with respect of the obtained valued for the neat CNF and LCNF films, respectively; and the WVTR was reduced by 16% and 35%, with respect to the values obtained for the neat CNF and LCNF films, respectively. Therefore, it can be concluded that there is a synergy between LCNF and CNF when combined in this formulation, and this may be ascribed to the lignin acting as chemical adhesive between CNF (Kang et al., 2019) and to the coexistence of nanofibrils of different diameter sizes which may create tortuous paths for gas molecules (Roohani, 2008) However, increasing the LCNF content in the bi-component CNF/LCNF 50 and CNF/LCNF 75 films, led to an increase in gas permeability. This fact is probably due to the decrease in the crystallinity and/or the larger size of the LCNF (Trifol et al., 2021), resulting in a lower packing density in fibrils (Table 2).

The mechanical properties of the materials are shown in Table 2. Neat CNF and LCNF films showed similar tensile mechanical properties to other nanocellulose films reported in the literature (Peng et al., 2011). In general, the addition of LCNF to the CNF in film formulations led to an improvement of the tensile strength and elongation. Residual lignin in LCNF has shown to decrease the number of effective hydrogen bonds between the nanofibrils (Amini et al., 2020) within the films, reducing both the tensile strength and modulus. However, in this study all the bio-component films displayed a higher tensile strength and an improved strain at break, comparing with the neat CNF films. Therefore, lignin is acting as a bonding agent imparting flexibility and transferring the load effectively between the different nanofibrils. Specifically, the incorporation of 25% of LCNF improved the strain at break by a factor of 4 and the stress at break by a factor of 2 when compared with neat CNF film. It is also noteworthy that increasing LCNF content above 25%, the young modulus and stress at break decreased with respect to the CNF/LCNF 25 films. These results may be explained from the increase in the pores or defects in the films due to a higher content of larger diameter cellulose nanofibrils. From those results, it can be speculated that the presence of moderate amounts of residual lignin (around 5%) in the films contributed to compatibilized the cellulose nanofibrils of both types of nanocelluloses, hence increasing the mechanical and barrier properties.

Table 2
Summary of the data from the tensile mechanical properties.

	Density (g/cm^3)[a]	Moisture uptake (%)[a]	E (GPa)[b]	σMPa)[c]	s (mm/mm)[d]
CNF	1.55	8.4 + /- 0.2	8.4 + /- 0.4	93.6 + / − 9.6	1.4 + /- 0.04
CNF/LCNF 25	1.45	9.3 + /- 0.3	7.2 + /- 0.4	182.8 + /- 5.7	5.8 + /- 0.8
CNF/LCNF 50	1.37	8.6 + / 0.2	6.7 + /- 0.5	152.1 + /- 28.9	4.7 + /- 1.8
CNF/LCNF 75	1.33	8.7 + /- 0.4	5.6 + /- 0.4	112.8 + /- 20.7	5.2 + /- 2.1
LCNF	1.32	9.1 + /- 0.4	3.8 + /- 0.3	122.6 + /- 4.8	6.4 + /- 0.3

[a] Measured at 23 °C and 50% RH.
[b] Young modulus.
[c] Stress at break.
[d] Strain at break.

4. Conclusions

In this work we have revalorized pine cone residues as films for packaging consisting in a combination of two different grades of nanocelluloses: cellulose nanofibers (CNF) and lignin containing cellulose nanofibrils (LCNF). These nanocellulose-based bicomponent films have shown better thermo-mechanical and functionality than the CNF neat films, showing therefore a higher potential than pure CNF for packaging applications. Specifically, it was found that the incorporation of small amounts (25%) of LCNF to CNF formulations in films:

- Substantially increased its mechanical properties (94% tensile stress and 414% strain at break).
- Decreased the oxygen transmission rate (OTR) by 53%.
- Decreased the water vapor transmission rate (WVTR) by 16%.
- Provided antioxidant properties.
- Provided UV-blocking behavior (94% decrease on transmittance at 320 nm) without significantly affecting transparency in the visible region.

HIgh mechanical strength and flexibility together with gas permeability can bring important target properties for packaging applications, i.e for barrier film food packaging and barrier coatings for papers and bioplastic packaging. Hence, the results of this study indicated the high potential of using an abundant worldwide available residual biomass as bio-based packaging solutions. This research will contribute therefore to achieve the sustainable goals and to develop a circular economy by eliminating wastes and maximizing the value of renewable resources.

CRediT authorship contribution statement

Jon Trifol. Conceptualization, Methodology, Formal analysis,

Writing – original draft, Writing – review and editing. **Rosana Moriana**. Conceptualization, Validation, Writing – original draft, Writing – review and editing, Supervision, Funding acquisition.

Declaration of Competing Interest

The authors declare the following financial interests/personal relationships which may be considered as potential competing interests: Jon Trifol reports financial support was provided by Academy of Finland. Jon Trifol reports financial support was provided by AForsk.

Acknowledgments

This research was supported by ÅForsk, project 18–316. JT acknowledges the Academy of Finland's Flagship Program under Projects No. 318890 and 318891 for its financial support.

References

Abdul Khalil, H.P.S.P.S., Davoudpour, Y., Saurabh, C.K., Hossain, M.S., Adnan, A.S., Dungani, R., Paridah, M.T.T., Mohamed, Z.I.S., Fazita, M.R.N.N., Syakir, M.I., Haafiz, M.K.M.K.M., Islam Sarker, M.Z., Fazita, M.R.N.N., Syakir, M.I., Haafiz, M.K. M.K.M., 2016. A review on nanocellulosic fibres as new material for sustainable packaging: process and applications. Renew. Sustain. Energy Rev. 64, 823–836. https://doi.org/10.1016/j.rser.2016.06.072.

Amini, E., Hafez, I., Tajvidi, M., Bousfield, D.W., 2020. Cellulose and lignocellulose nanofibril suspensions and films: a comparison. Carbohydr. Polym. 250, 117011 https://doi.org/10.1016/j.carbpol.2020.117011.

Aulin, C., Salazar-Alvarez, G., Lindström, T., 2012. High strength, flexible and transparent nanofibrillated cellulose-nanoclay biohybrid films with tunable oxygen and water vapor permeability. Nanoscale 4, 6622–6628. https://doi.org/10.1039/c2nr31726e.

Azeredo, H.M.C., Rosa, M.F., Mattoso, L.H.C., 2017. Nanocellulose in bio-based food packaging applications. Ind. Crops Prod. 97, 664–671. https://doi.org/10.1016/j.indcrop.2016.03.013.

Baniasadi, H., Trifol, J., Ranta, A., Seppälä, J., 2021. Exfoliated clay nanocomposites of renewable long-chain aliphatic polyamide through in-situ polymerization. Compos. Part B Eng. 211, 108655 https://doi.org/10.1016/j.compositesb.2021.108655.

Bian, H., Chen, L., Dong, M., Wang, L., Wang, R., Zhou, X., Wu, C., Wang, X., Ji, X., Dai, H., 2021. Natural lignocellulosic nanofibril film with excellent ultraviolet blocking performance and robust environment resistance. Int. J. Biol. Macromol. 166, 1578–1585. https://doi.org/10.1016/j.ijbiomac.2020.11.037.

Catignani, G., Carter, M.E., 1982. Antioxidant properties of lignin. J. Food Sci. 47 https://doi.org/10.1111/j.1365-2621.1982.tb05029.x (1745–1745).

Chen, Y., Fan, D., Han, Y., Lyu, S., Lu, Y., Li, G., Jiang, F., Wang, S., 2018. Effect of high residual lignin on the properties of cellulose nanofibrils/films. Cellulose 25, 6421–6431. https://doi.org/10.1007/s10570-018-2006-x.

Cherian, B.M., Leão, A.L., De Souza, S.F., Costa, L.M.M., De Olyveira, G.M., Kottaisamy, M., Nagarajan, E.R., Thomas, S., 2011. Cellulose nanocomposites with nanofibres isolated from pineapple leaf fibers for medical applications. Carbohydr. Polym. 86, 1790–1798. https://doi.org/10.1016/j.carbpol.2011.07.009.

España, J.M., Fages, E., Moriana, R., Boronat, T., Balart, R., 2012. Antioxidant and antibacterial effects of natural phenolic compounds on green composite materials. Polym. Compos. 33, 1288–1294. https://doi.org/10.1002/pc.22254.

Fukuzumi, H., Saito, T., Iwata, T., Kumamoto, Y., Isogai, A., 2009. Transparent and high gas barrier films of cellulose nanofibers prepared by TEMPO-mediated oxidation. Biomacromolecules 10, 162–165. https://doi.org/10.1021/bm801065u.

Georgouvelas, D., Jalvo, B., Valencia, L., Papawassiliou, W., Pell, A.J., Edlund, U., Mathew, A.P., 2020. Residual lignin and Zwitterionic polymer grafts on cellulose nanocrystals for antifouling and antibacterial applications. ACS Appl. Polym. Mater. 2, 3060–3071. https://doi.org/10.1021/acsapm.0c00212.

Hansen, Plackett, 2008. Sustainable Films and Coatings from Hemicelluloses: A Review. Biomacromolecules 9, 1493–1505. https://doi.org/10.1021/bm800053z.

Herrera, M., Thitiwutthisakul, K., Yang, X., Rujitanaroj, P. on, Rojas, R., Berglund, L., 2018. Preparation and evaluation of high-lignin content cellulose nanofibrils from eucalyptus pulp. Cellulose 25, 3121–3133. https://doi.org/10.1007/s10570-018-1764-9.

Horseman, T., Tajvidi, M., Diop, C.I.K., Gardner, D.J., 2017. Preparation and property assessment of neat lignocellulose nanofibrils (LCNF) and their composite films. Cellulose 24, 2455–2468. https://doi.org/10.1007/s10570-017-1266-1.

Kang, X., Kirui, A., Dickwella Widanage, M.C., Mentink-Vigier, F., Cosgrove, D.J., Wang, T., 2019. Lignin-polysaccharide interactions in plant secondary cell walls revealed by solid-state NMR. Nat. Commun. 10, 347. https://doi.org/10.1038/s41467-018-08252-0.

Lavoine, N., Desloges, I., Dufresne, A., Bras, J., 2012. Microfibrillated cellulose – its barrier properties and applications in cellulosic materials: a review. Carbohydr. Polym. 90, 735–764. https://doi.org/10.1016/j.carbpol.2012.05.026.

Le Normand, M., Moriana, R., Ek, M., 2014. The bark biorefinery: a side- stream from the forest industry converted into nanocomposites with high oxygen barrier. Cellulose 21, 4583–4594.

Li, D., Moriana, R., Ek, M., 2016. From forest wastes to added value products: using a green oxygen-barrier coating from birch bark on nanocomposites derived from spruce residues. Nord. Pulp Pap. J. Res. 31.

Liu, A., Berglund, L.A., 2012. Clay nanopaper composites of nacre-like structure based on montmorrilonite and cellulose nanofibers – improvements due to chitosan addition. Carbohydr. Polym. 87, 53–60. https://doi.org/10.1016/j.carbpol.2011.07.019.

Mehta, M.J., Kumar, A., 2019. Ionic liquid stabilized gelatin–lignin films: a potential UV-shielding material with excellent mechanical and antimicrobial properties. Chem. - A Eur. J. 25, 1269–1274. https://doi.org/10.1002/chem.201803763.

Minelli, M., Baschetti, M.G., Doghieri, F., Ankerfors, M., Lindström, T., Siró, I., Plackett, D., 2010. Investigation of mass transport properties of microfibrillated cellulose (MFC) films. J. Membr. Sci. 358, 67–75. https://doi.org/10.1016/j.memsci.2010.04.030.

Missoum, K., Belgacem, M.N., Bras, J., 2013. Nanofibrillated cellulose surface modification: a review. Materials 6, 1745–1766. https://doi.org/10.3390/ma6051745.

Oinonen, P., Krawczyk, H., Ek, M., Henriksson, G., Moriana, R., 2016. Bioinspired composites from cross-linked galactoglucomannan and microfibrillated cellulose: thermal, mechanical and oxygen barrier properties. Carbohydr. Polym. 136, 146–153. https://doi.org/10.1016/j.carbpol.2015.09.038.

Peng, X., Ren, J., Zhong, L., Sun, R.-C., 2011. Nanocomposite films based on xylan-rich hemicelluloses and cellulose nanofibres with enhanced mechanical properties. Biomacromolecules 12, 3321–3329. https://doi.org/10.1021/bm2008795.

Rodionova, G., Lenes, M., Eriksen, O., Gregersen, O., 2011. Surface chemical modification of microfibrillated cellulose: improvement of barrier properties for packaging applications. 18, 127–134.

Rojo, E., Peresin, M.S., Sampson, W.W., Hoeger, I.C., Vartiainen, J., Laine, J., Rojas, O.J., 2015. Comprehensive elucidation of the effect of residual lignin on the physical, barrier, mechanical and surface properties of nanocellulose films. Green Chem. 17, 1853–1866. https://doi.org/10.1039/c4gc02398f.

Roohani, et al., 2008. Cellulose whiskers reinforced polyvinyl alcohol copolymers nanocomposites. European Polymer Journal 44 (8).

Schmid, M., Kerstin, D., Bugnicourt, E., Cordoni, D., Wild, F., Lazzeri, A., Noller, K., 2012. Properties of whey-protein-coated films and laminates as novel recyclable food packaging materials with excellent barrier properties. Int. J. Polym. Sci. 12, 7. https://doi.org/10.1155/2012/562381.

Segal, L., Creely, J.J., Martin, A.E., Conrad, C.M., 1959. An empirical method for estimating the degree of crystallinity of native cellulose using the X-ray diffractometer. Text. Res. J. 29, 786–794. https://doi.org/10.1177/004051755902901003.

Shimazdu Corporation, 2016. How can I determine the haze value of a resin sheet or film? [WWW Document]. Appl. News.

Siró, I., Plackett, D., 2010. Microfibrillated cellulose and new nanocomposite materials: a review. Cellulose 17, 459–494. https://doi.org/10.1007/s10570-010-9405-y.

Sorrentino, A., Gorrasi, G., Vittoria, V., 2007. Potential perspectives of bio-nanocomposites for food packaging applications. Trends Food Sci. Technol. 18, 84–95. https://doi.org/10.1016/j.tifs.2006.09.004.

Svärd, A., Moriana, R., Brännvall, E., Edlund, U., 2019. Rapeseed straw biorefinery process. ACS Sustain. Chem. Eng. 7, 790–801. https://doi.org/10.1021/acssuschemeng.8b04420.

Tagami, A., Gioia, C., Lauberts, M., Budnyak, T., Moriana, R., Lindström, M.E., Sevastyanova, O., 2019. Solvent fractionation of softwood and hardwood kraft lignins for more efficient uses: compositional, structural, thermal, antioxidant and adsorption properties. Ind. Crops Prod. 129, 123–134. https://doi.org/10.1016/j.indcrop.2018.11.067.

Trifol, J., Plackett, D., Sillard, C., Hassager, O., Daugaard, A.E., Bras, J., Szabo, P., 2016a. A comparison of partially acetylated nanocellulose, nanocrystalline cellulose, and nanoclay as fillers for high-performance polylactide nanocomposites. J. Appl. Polym. Sci. 133, 1–14. https://doi.org/10.1002/app.43257.

Trifol, J., Plackett, D., Sillard, C., Szabo, P., Bras, J., Daugaard, A.E., 2016b. Hybrid poly (lactic acid)/nanocellulose/nanoclay composites with synergistically enhanced barrier properties and improved thermomechanical resistance. Polym. Int. 65, 988–995. https://doi.org/10.1002/pi.5154.

Trifol, J., Sillard, C., Plackett, D., Szabo, P., Bras, J., Daugaard, A.E., 2017. Chemically extracted nanocellulose from sisal fibres by a simple and industrially relevant process. Cellulose 24, 107–118. https://doi.org/10.1007/s10570-016-1097-5.

Trifol, J., van Drongelen, M., Clegg, F., Plackett, D., Szabo, P., Daugaard, A.E., 2019. Impact of thermal processing or solvent casting upon crystallization of PLA nanocellulose and/or nanoclay composites. J. Appl. Polym. Sci. 47486, 47486. https://doi.org/10.1002/app.47486.

Trifol, J., Marin Quintero, D.C., Moriana, R., 2021. Pine cone biorefinery: integral valorization of residual biomass into lignocellulose nanofibrils (LCNF)-reinforced composites for packaging. ACS Sustain. Chem. Eng. 9, 2180–2190. https://doi.org/10.1021/acssuschemeng.0c07687.

Tsuji, H., Okino, R., Daimon, H., Fujie, K., 2006. Water vapor permeability of poly (lactide)s: effects of molecular characteristics and crystallinity. J. Appl. Polym. Sci. 99, 2245–2252. https://doi.org/10.1002/app.22698.

Yang, S., Wang, T., Tang, R., Yan, Q., Tian, W., Zhang, L., 2020. Enhanced permeability, mechanical and antibacterial properties of cellulose acetate ultrafiltration membranes incorporated with lignocellulose nanofibrils. Int. J. Biol. Macromol. 151, 159–167. https://doi.org/10.1016/j.ijbiomac.2020.02.124.